



# A new perfluorinated peroxy nitrates, $\text{CF}_3\text{CF}_2\text{CF}_2\text{CF}_2\text{OONO}_2$ . Synthesis, characterization and atmospheric implications



Adriana G. Bossolasco, Jesús A. Vila, Maxi A. Burgos Paci, Fabio E. Malanca\*, Gustavo A. Argüello

Instituto de Investigaciones en Físicoquímica de Córdoba (INFIQC), CONICET – Departamento de Físicoquímica, Facultad de Ciencias Químicas (Universidad Nacional de Córdoba), Ciudad Universitaria, X5000HUA Córdoba, Argentina

## ARTICLE INFO

### Article history:

Received 3 April 2014

In final form 16 June 2014

Available online 2 July 2014

### Keywords:

Perfluoro alkyl peroxy nitrates

$\text{CF}_3\text{CF}_2\text{CF}_2\text{CF}_2\text{OONO}_2$

Thermal decomposition

Kinetic parameters

## ABSTRACT

$\text{CF}_3\text{CF}_2\text{CF}_2\text{CF}_2\text{OONO}_2$  was synthesized from the photolysis of  $\text{CF}_3\text{CF}_2\text{CF}_2\text{CF}_2\text{I}$ , in presence of  $\text{NO}_2$  and  $\text{O}_2$ . Alkyl peroxy nitrates ( $\text{C}_x\text{F}_{2x+1}\text{OONO}_2$ ) could be formed in the atmospheric degradation of chlorofluorocarbons, hydrofluorocarbons and hydrofluoroethers. We present here the synthesis and characterization (IR and UV absorption cross sections) of  $\text{CF}_3\text{CF}_2\text{CF}_2\text{CF}_2\text{OONO}_2$  and its comparison with those corresponding to other perfluoro alkyl peroxy nitrates. The thermal stability was studied as a function of total pressure (from 9.0 to 417 mbar) and temperature (from 283 to 293 K) using infrared spectroscopy. Kinetic parameters measured for the thermal dissociation were  $E_a = (81 \pm 4) \text{ kJ/mol}$  and  $A = 4.8 \times 10^{12}$ . DFT calculations at the B3LYP/6-311+G\* level were used to explore the ground state potential energy surface. Geometrical parameters, conformer populations and vibrational spectra are presented. The calculated activation energy was  $81.3 \text{ kJ mol}^{-1}$  in excellent agreement with experimental results. Atmospheric implications are discussed.

© 2014 Elsevier B.V. All rights reserved.

## 1. Introduction

Peroxy nitrates are formed in the degradation of volatile compounds emitted to the atmosphere, and are important reservoirs of peroxy radicals and  $\text{NO}_2$ . Precisely due to their stability (from hours to days in the free atmosphere), they can reach higher altitudes where lower temperatures stabilize the molecules and consequently they can be transported to remote places [1–3].

The loss of peroxy nitrates in the atmosphere occurs through different processes, namely thermal decomposition, photolysis, and reaction with OH radicals, whose relative importance depends on the region of the atmosphere and the nature of the peroxy nitrates [4–7]. Perfluoro acyl ( $\text{C}_x\text{F}_{2x+1}\text{C(O)OONO}_2$ ) and perfluoro alkyl ( $\text{C}_x\text{F}_{2x+1}\text{OONO}_2$ ) peroxy nitrates are important families that could be formed in the degradation of a series of compounds used as refrigerants, blowing and cleaning agents, emulsifiers and solvents [8–11]. In particular, the degradation of n- $\text{CF}_3\text{CF}_2\text{CF}_2\text{CF}_2\text{H}$  (HFC-329p), an HFC with a lifetime of 33 years, leads to perfluorinated radicals,  $\text{CF}_3\text{CF}_2\text{CF}_2\text{CF}_2$  [12], and subsequent reactions with  $\text{O}_2$  and  $\text{NO}_2$  could give rise to the corresponding perfluoro alkyl peroxy nitrates,  $\text{CF}_3\text{CF}_2\text{CF}_2\text{CF}_2\text{OONO}_2$ . Previous studies reported the synthesis and characterization, thermal stability, UV and infrared

spectra and atmospheric lifetimes for perfluoro alkyl peroxy nitrates ( $\text{C}_x\text{F}_{2x+1}\text{OONO}_2$ ), with  $x = 1$  [8,13–15] and  $x = 2, 3$  [16,11]. Within this context, we present here the synthesis of the perfluoro n-butyl peroxy nitrates ( $\text{CF}_3\text{CF}_2\text{CF}_2\text{CF}_2\text{OONO}_2$ ) as well as its characterization to extend the study of this family.

$\text{CF}_3\text{CF}_2\text{CF}_2\text{CF}_2\text{OONO}_2$  was formed by the reaction between  $\text{CF}_3\text{CF}_2\text{CF}_2\text{CF}_2$  radicals and  $\text{O}_2$  (Reaction (1))



followed by the reaction with  $\text{NO}_2$  (Reaction (2))



Our results provided infrared and ultraviolet spectra, thermal stability – as a function of the temperature and pressure – and atmospheric lifetimes – as a function of altitude.

## 2. Experimental

### 2.1. Photochemical synthesis of $\text{CF}_3\text{CF}_2\text{CF}_2\text{CF}_2\text{OONO}_2$

Commercially available samples of  $\text{CF}_3\text{CF}_2\text{CF}_2\text{CF}_2\text{I}$  (Sigma–Aldrich),  $\text{O}_2$  (AGA) and  $\text{NO}$  (AGA) were used, all of them with a purity higher than 98%.  $\text{NO}_2$  was prepared adding  $\text{O}_2$  to  $\text{NO}$  with further purification obtaining a sample with 99% purity. Volatile

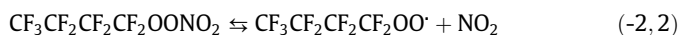
\* Corresponding author. Tel.: +54 3515353866.

E-mail address: [fmalanca@fcq.unc.edu.ar](mailto:fmalanca@fcq.unc.edu.ar) (F.E. Malanca).

materials and gases were manipulated in a conventional glass vacuum line.

Perfluoro n-butyl peroxyxynitrate was synthesized by the photolysis of mixtures containing perfluoro n-butyl iodide,  $\text{CF}_3\text{CF}_2\text{CF}_2\text{CF}_2\text{I}$ , (7.0 mbar),  $\text{NO}_2$  (3.5 mbar) and  $\text{O}_2$  (1000 mbar) in a 12 L reactor using an internal 40 W low pressure mercury lamp ( $\lambda_{\text{max}} = 254 \text{ nm}$ ) located in a double walled quartz jacket through which flowing water maintained constant temperature. The procedure to synthesize the  $\text{CF}_3\text{CF}_2\text{CF}_2\text{CF}_2\text{OONO}_2$  was similar to that used by Mayer-Figge et al. for  $\text{CF}_3\text{OONO}_2$  [13]. The quartz jacket closed the 12 L glass reactor through a tapered joint and the photolyses were carried out maintaining the temperature at 278 K to minimize the thermal decomposition of  $\text{CF}_3\text{CF}_2\text{CF}_2\text{CF}_2\text{OONO}_2$ .

The progress of the synthesis was monitored by infrared spectroscopy (Bruker IFS 66v FTIR Spectrometer) using a standard infrared gas cell (optical path,  $l = 23 \text{ cm}$ ), by taking small fractions of the mixture every 5 min. The irradiation was stopped when the  $\text{NO}_2$  signal decreased to one third of the initial value ( $\sim 30 \text{ min}$ ), to assure that  $\text{NO}_2$  concentration is still sufficiently high to prevent the decomposition of the peroxyxynitrate (Reaction (-2)) and to shift the equilibrium to the re-formation of the peroxyxynitrate:



The resultant mixture of photolysis was collected by slowly passing it through three traps kept at 77 K in order to remove excess  $\text{O}_2$ . It was then distilled trap to trap between 188 and 153 K to eliminate the  $\text{CF}_2\text{O}$ . Further distillation using three traps at 213, 193 and 173 K allows obtaining  $\text{CF}_3\text{CF}_2\text{CF}_2\text{CF}_2\text{OONO}_2$  in the fraction at 173 K.

## 2.2. IR and UV spectroscopy

The experimental IR and UV absorption cross sections were obtained from measurements of absorbances at 300 K, according to Eq. (3)

$$\sigma(\text{cm}^2 \text{ molec}^{-1}) = \frac{\text{Abs} \times T(\text{K}) \times 31, 7 \times 10^{-20}}{p(\text{mbar}) \times l(\text{cm})} \quad (3)$$

where “ $p$ ” denotes the pressure, and “ $T$ ” the temperature. The pressures of  $\text{CF}_3\text{CF}_2\text{CF}_2\text{CF}_2\text{OONO}_2$  ranged from 0.5 to 3.0 mbar, and the cross sections were conveniently averaged. Infrared spectra were recorded with a resolution of  $2 \text{ cm}^{-1}$  averaging 16 scans in the range of  $4000\text{--}400 \text{ cm}^{-1}$ . UV spectra were recorded from 200 to 282 nm with a resolution of 1 nm.

## 3. Computational details

Density functional theory has been used to evaluate the ground state geometrical parameters, vibrational frequencies and the thermal populations of many of the conformers of  $\text{CF}_3\text{CF}_2\text{CF}_2\text{CF}_2\text{OONO}_2$ . The hybrid density functional B3LYP with the 6-311+G\* basis set was employed in all calculations. DFT methods have been extensively employed to describe fluoro-oxygenated systems showing acceptable precision [17–19]. Only minimum points of the potential energy surface (PES) were explored, confirmed by no imaginary frequencies in the hessian matrix.

When using first principle calculations without explicit treatment of correlation energy to describe bond breaking processes, the spin contamination from the generated radicals would cause significant errors in the computed energies. To attenuate this effect unrestricted wavefunctions and mixing of the Homo–Lumo molecular orbitals were employed to study the RO– $\text{NO}_2$  bond fission. Calculations were run without symmetry restrictions. The G09 program package [20] in conjunction with GaussView 5.0 [21] were

employed. The vibrational frequencies informed were taken from the G09 output without additional corrections.

## 3.1. Thermal decomposition

Thermal decompositions of  $\text{CF}_3\text{CF}_2\text{CF}_2\text{CF}_2\text{OONO}_2$  were carried out at temperatures ranging between 283 and 293 K, adding NO (3.0 mbar) to prevent the occurrence of reaction (2) through the capture of the peroxy radicals formed



as done for other peroxy radicals [22], and monitoring the temporal variation of the peroxyxynitrate by infrared spectroscopy. The pressure was set from 9.0 to 417 mbar, adding He in order to study the pressure dependence.

## 4. Results and discussion

### 4.1. Photochemical synthesis of $\text{CF}_3\text{CF}_2\text{CF}_2\text{CF}_2\text{OONO}_2$

Fig. 1 shows the mixture at  $t = 0 \text{ min}$  (upper trace) and  $t = 30 \text{ min}$  irradiation (second trace), and the sequence of spectra used to identify the products of the synthesis. The third trace, which corresponds to the products, was obtained by subtraction of reference spectra for  $\text{CF}_3\text{CF}_2\text{CF}_2\text{CF}_2\text{I}$  and  $\text{NO}_2$  to the second one. It is clear the appearance of peaks corresponding to carbonyl fluoride ( $\text{CF}_2\text{O}$ ), and perfluoro alkyl peroxyxynitrates (signals at  $1764$  and  $790 \text{ cm}^{-1}$ ). Being so evident the formation of  $\text{CF}_2\text{O}$ , there should have formed also a species with less than four carbon atoms. The most likely candidate is  $\text{CF}_3\text{CF}_2\text{CF}_2\text{OONO}_2$ ; therefore subtraction of the spectra of  $\text{CF}_2\text{O}$  and  $\text{CF}_3\text{CF}_2\text{CF}_2\text{OONO}_2$  (from our repository of pure substances [11]) reveals the formation of a new peroxyxynitrate, which was assigned to  $\text{CF}_3\text{CF}_2\text{CF}_2\text{CF}_2\text{OONO}_2$ , as will be discussed below.

The carbonyl fluoride ( $\text{CF}_2\text{O}$ ) and  $\text{CF}_3\text{CF}_2\text{CF}_2\text{OONO}_2$  formed (though in moderate quantities,  $\sim 9\%$ ), are a consequence of a series of reactions initiated by the slow thermal decomposition of  $\text{CF}_3\text{CF}_2\text{CF}_2\text{CF}_2\text{OONO}_2$ . The peroxy radicals formed by reaction (-2) could either react with NO (originated from the photolysis of  $\text{NO}_2$ ,  $\sigma_{254 \text{ nm}} = 1.08 \pm 0.07 \times 10^{-20} \text{ cm}^2 \text{ molecule}^{-1}$ ), iodine atoms ( $k = (3.7 \pm 0.8) \times 10^{-11} \text{ cm}^3 \text{ molecule}^{-1} \text{ s}^{-1}$ ) consequence of the

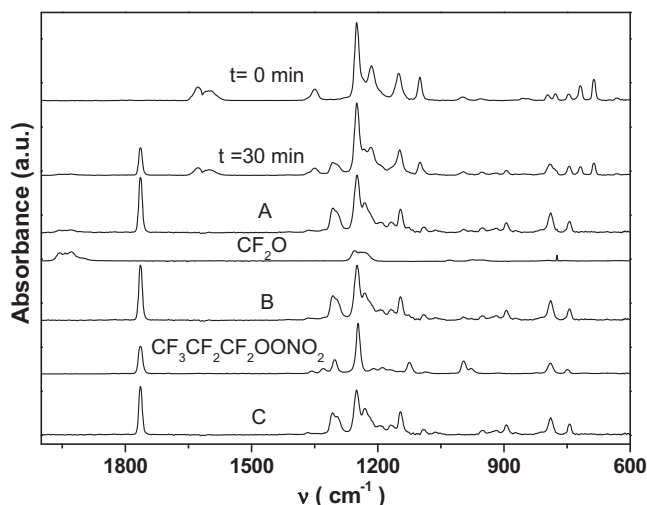


Fig. 1. Photolysis of  $\text{CF}_3\text{CF}_2\text{CF}_2\text{CF}_2\text{I}$  in the presence of  $\text{NO}_2$  and  $\text{O}_2$ . From top to bottom: before photolysis; after 30 min of irradiation; products (A);  $\text{CF}_2\text{O}$  reference spectrum; A minus  $\text{CF}_2\text{O}$  (B);  $\text{CF}_3\text{CF}_2\text{CF}_2\text{OONO}_2$  reference spectrum; and B minus  $\text{CF}_3\text{CF}_2\text{CF}_2\text{OONO}_2$  (C).

photochemical rupture of the precursor ( $\sigma_{254\text{ nm}} = (3.86 \pm 0.07) \times 10^{-19} \text{ cm}^2 \text{ molecule}^{-1}$ ) [23], or recombine to give  $\text{CF}_3\text{CF}_2\text{CF}_2\text{CF}_2\text{O}^\bullet$  radicals, which in turn decompose as in reaction (5)



The  $\text{CF}_3\text{CF}_2\text{CF}_2^\bullet$  radicals lead finally to the formation of  $\text{CF}_3\text{CF}_2\text{CF}_2\text{OONO}_2$  following the established sequence of reactions with  $\text{O}_2$  and  $\text{NO}_2$ . The complete mechanism reaction is presented in Fig. 2.

#### 4.2. DFT calculations

The conformational space of  $\text{CF}_3\text{CF}_2\text{CF}_2\text{CF}_2\text{OONO}_2$  has been studied taking into account the six main dihedral angles of the skeleton  $\text{F}-\text{CF}_2-\text{CF}_2-\text{CF}_2-\text{CF}_2-\text{O}-\text{O}-\text{N}-\text{O}$ , which can be reduced to four according to what follows. Previous studies for similar peroxy nitrates [11,14] have shown that  $\varphi_1(\text{F}-\text{CF}_2-\text{CF}_2-\text{CF}_2)$  always adopts the *anti* configuration and  $\varphi_6(\text{O}-\text{O}-\text{N}-\text{O})$  the *syn* one. The four remaining dihedrals are:  $\varphi_2(\text{CF}_2-\text{CF}_2-\text{CF}_2-\text{CF}_2)$  which is the carbon skeleton configuration;  $\varphi_3(\text{F}_2\text{C}-\text{CF}_2-\text{CF}_2-\text{O})$  which sets the relative position of the  $\text{C}_3\text{F}_7$  fragment respect to the peroxy bond;  $\varphi_4(\text{CF}_2-\text{CF}_2-\text{O}-\text{O})$  and  $\varphi_5(\text{CF}_2-\text{O}-\text{O}-\text{N})$ .

Four different minima are found in the PES being the one with  $\varphi_2 = 165^\circ$ ;  $\varphi_3 = 54^\circ$ ;  $\varphi_4 = 180^\circ$  and  $\varphi_5 = 104^\circ$ , the global minimum. These four minima are designated from **1** to **4** in ascending order of their relative energy, as is shown in Table 1. Fig. 3 depicts the most stable rotamer along with the numbering of atoms. A qualitative inspection of the PES shows that inter-conversion between the minima could involve trajectories needing less than 4 kcal mol<sup>-1</sup>, and that the relative energies are less than 1.8 kcal mol<sup>-1</sup> relative to **1**. Table 1 shows the B3LYP/6-311+G\* absolute and relative energies together with the room temperature populations for the rotamers along with their corresponding partition functions. Relative populations were calculated according to the formula

$$N_1/N_x = Q_1/Q_x \cdot \exp(-\Delta E/kT) \quad (6)$$

where  $Q_x$  is the total partition function, taken from G09, of rotamer  $x$ . The  $Q_x$  values are calculated within the rigid-rotor/harmonic-oscillator model and the contribution of internal rotational modes are neglected. It is noteworthy that the calculation anticipates a blend of the four rotamers at room temperature. This will be confirmed when analyzing the IR spectrum. Table 2 shows the geometrical parameters for rotamer **1** together with values for  $\text{C}_3\text{F}_7\text{OONO}_2$  [11] calculated at the same level as well as the experimental GED results of  $\text{CF}_3\text{OONO}_2$  [14]. The  $\text{C}-\text{O}-\text{O}-\text{N}$  dihedral and the  $\text{O}-\text{N}$  distance are the two most interesting parameters in peroxy nitrates. There is strong experimental evidence showing that the dihedral  $\text{X}-\text{O}-\text{O}-\text{Y}$  decreases from  $\sim 120^\circ$  when X and Y are  $\text{sp}^3$  hybridized atoms to  $\sim 105^\circ$  when one is  $\text{sp}^3$  one  $\text{sp}^2$  and to  $\sim 90^\circ$  when both are

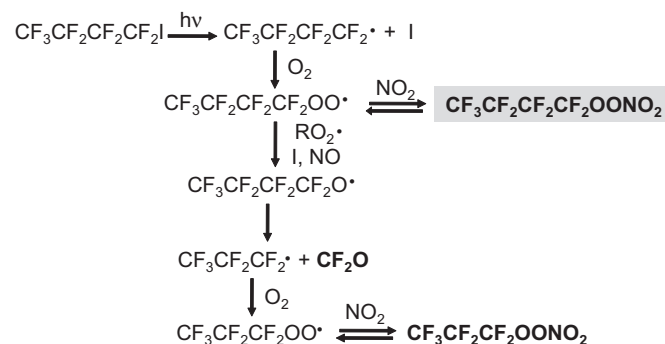


Fig. 2. Reaction mechanism for the photolysis of  $\text{CF}_3\text{CF}_2\text{CF}_2\text{CF}_2\text{I}$  in the presence of  $\text{NO}_2$  and  $\text{O}_2$ . Products formed are marked in bold, and the new peroxy nitrates formed is highlighted.

$\text{sp}^2$  [8,11,14]. The calculated value of this parameter is  $104.7^\circ$  for  $\text{C}_4\text{F}_9\text{OONO}_2$  and it is in perfect agreement with this tendency. The  $\text{O}-\text{N}$  distance is extremely long in peroxy nitrates and it has been observed that it depends on the electronegativity of the group attached to the  $-\text{ONO}_2$  fragment. Reported values of 1.507 and 1.523 Å are found for  $\text{FONO}_2$  and  $\text{CF}_3\text{OONO}_2$  respectively [14,24]. In the case of  $\text{C}_4\text{F}_9\text{OONO}_2$  a value of 1.561 Å is found, which is almost the same as for  $\text{C}_3\text{F}_7\text{OONO}_2$  within the calculated uncertainty, and larger than the experimental value for  $\text{CF}_3\text{OONO}_2$ . A separate DFT calculation for  $\text{CF}_3\text{OONO}_2$ ,  $\text{C}_2\text{F}_5\text{OONO}_2$  and  $\text{C}_3\text{F}_7\text{OONO}_2$  with the same basis set gives 1.560 Å for the  $\text{O}-\text{N}$  distance, showing that addition of  $\text{CF}_2$  groups to the carbon chain does not influence the  $\text{O}-\text{N}$  distance at the B3LYP/6-311+G\* method level. It can also be mentioned that this method overestimates the  $\text{O}-\text{N}$  distance when it is compared with the experimental value for  $\text{CF}_3\text{OONO}_2$  (1.523 Å). Unfortunately there are not experimental studies for the evaluation of the geometries of the series  $\text{C}_x\text{F}_{2x+1}\text{OONO}_2$  with  $x = 2-4$  and therefore these studies would have a lot of worth.

#### 4.3. IR and UV spectroscopy

Fig. 4 shows the experimental (a) and calculated (b) infrared spectra of  $\text{C}_4\text{F}_9\text{OONO}_2$ . The infrared bands (in units of  $\text{cm}^{-1}$ ), the corresponding absorbance cross sections ( $\sigma \times 10^{18} \text{ cm}^2 \text{ molecule}^{-1}$ , base e), and their assignment for the main peaks are: 1764 ( $3.51 \pm 0.07$ )  $\nu_{\text{as}}(\text{NO}_2)$ , 1307 ( $1.63 \pm 0.04$ )  $\nu_{\text{s}}(\text{NO}_2)$ , 1250 ( $3.36 \pm 0.07$ )  $\nu_{\text{as}}(\text{CF}_3)$ , 1145 ( $1.76 \pm 0.04$ )  $\nu_{\text{as}}(\text{C}-\text{F})$ , 894 ( $0.72 \pm 0.03$ )  $\nu_{\text{s}}(\text{O}-\text{O})$ , 789 ( $1.25 \pm 0.03$ )  $\delta_{\text{NO}_2}$ . These are in agreement with the general trend shown by many perfluoro alkyl peroxy nitrates ( $\text{C}_x\text{F}_{2x+1}\text{OONO}_2$ ,  $x = 1, 2, 3$ ) [11,13,16], that show rather narrow spans for the different IR bands as can be seen for  $\nu_{\text{as}}-\text{NO}_2$  (1764–1762  $\text{cm}^{-1}$ ),  $\nu_{\text{as}}-\text{CF}_3$  (1244–1250  $\text{cm}^{-1}$ ), and  $\delta_{\text{NO}_2}$  (789–792  $\text{cm}^{-1}$ ). A comparison between the experimental and theoretical spectra shows a remarkable agreement, both in the relative intensities as well as in the position of the main peaks. Notice that all the experimental bands have their calculated counterpart, thus corroborating the identity of the new peroxy nitrates.

As stated before, four different rotamers should be in equilibrium in a gas phase sample of  $\text{CF}_3\text{CF}_2\text{CF}_2\text{CF}_2\text{OONO}_2$  at room temperature, according to the DFT calculation. Because of this, the theoretical spectrum shown in the bottom of Fig. 4 was the result of the linear combination of the theoretical spectrum of each rotamer multiplied by the corresponding population. Every vibrational transition was modeled with a Lorentzian function with 4  $\text{cm}^{-1}$  of FWHM. The comparison between the experimental and theoretical spectra shows an excellent correlation for the featured peaks.

Table 3 shows the UV absorption cross sections determined in our work for  $\text{CF}_3\text{CF}_2\text{CF}_2\text{CF}_2\text{OONO}_2$  from 200 to 282 nm, and their comparison with data obtained from literature [11,15] for perfluoro alkyl peroxy nitrates of shorter carbon chains,  $\text{C}_x\text{F}_{2x+1}\text{OONO}_2$  ( $x = 1, 3$ ). The absorption cross sections were the average of five spectra from samples ranging from 1.0 to 3.2 mbar that contained the unavoidable small quantities of  $\text{NO}_2$ , whose absorbances were conveniently subtracted using the absorption cross sections recommended in Sander et al. [25].

The comparison of the cross sections for the peroxy nitrates corroborates the general trend that shows a consistent decrease as the length of the carbonated chain increases, probably as a consequence of the increment of the number of  $\text{CF}_2$  groups and the concomitant increase in their withdrawing capacity.

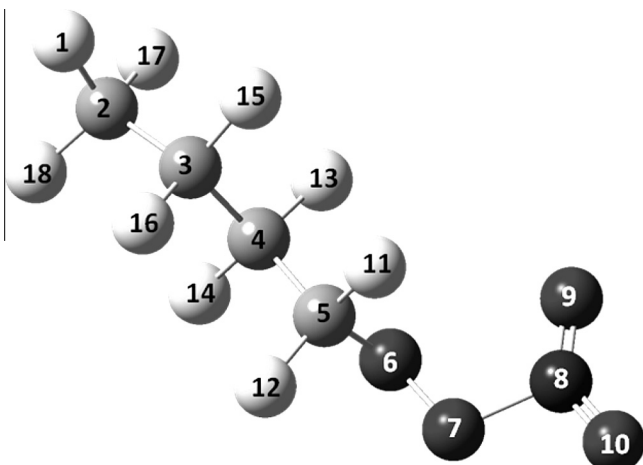
#### 4.4. Thermal stability

The thermal stability of  $\text{CF}_3\text{CF}_2\text{CF}_2\text{CF}_2\text{OONO}_2$  was studied at different temperatures and total pressures, always in the presence of

**Table 1**

B3LYP/6-311+G\* absolute energies plus ZPE, relative energies, partition function and room temperature populations for the different rotamers.

Conformer		Energy (Ha)	$\Delta E$ (kcal/mol)	Q	Population
1	165-54-180-104	-1406.837801	0	$2.87 \cdot 10^{21}$	0.63
2	166-170-180-104	-1406.836962	0.53	$3.01 \cdot 10^{21}$	0.27
3	64-48-180-109	-1406.835759	1.14	$1.48 \cdot 10^{21}$	0.04
4	60-56-180-107	-1406.835991	1.28	$1.75 \cdot 10^{21}$	0.06

**Fig. 3.** Calculated structure for the most stable conformer of  $C_4F_9OONO_2$  (1).

NO to remove the  $CF_3CF_2CF_2CF_2OO\cdot$  radicals thus allowing the determination of the rate constant for the thermal decomposition.

The rate coefficients for reaction (-2) were corrected considering that, as time elapses, the NO added leads to an increase in  $NO_2$  formation, slightly shifting the equilibrium toward the formation of  $CF_3CF_2CF_2OONO_2$  via reaction (2). The equation used to correct the rate coefficient

$$k_{-2} = k_{OBS} \left( 1 + \frac{k_2 [NO_2]}{k_4 [NO]} \right) \quad (7)$$

has been profusely used [26–28] even though in many cases it was necessary to resort to values for similar entities because the

unavailability of proper data. The rate constants for reactions (2) and (4) were assumed equal to those determined for  $CF_3CF_2CF_2CF_2OO\cdot$  radicals [29]. The rate constants reported and the typical concentrations of  $NO_2$  and  $NO$  in our experiments provide a value of 1.04 for the bracketed term in Eq. (7), leading to a correction of 4%. The values obtained for the rate constant  $k_{-2}$ , and its dependence with temperature and pressure, are presented in Fig. 5. Temporal variation of  $CF_3CF_2CF_2CF_2OONO_2$  was monitored using the peak at  $1764 \text{ cm}^{-1}$ . Errors bars included in the figure were obtained from the fitting of the experimental data by linear regression.

The Arrhenius plot was obtained at 9.0 mbar of total pressure from 283 to 293 K. The kinetic parameters determined,  $E_a = (81 \pm 4) \text{ kJ/mol}$  and  $A = 3.2 \times 10^{12}$  ( $\ln A = 29 \pm 2$ ) for  $C_xF_{2x+1}OONO_2$  ( $x = 4$ ), as well as those taken from Mayer et al. [13] ( $x = 1$ ) and Bossolasco et al. [11,16] ( $x = 2, 3$ ) allow the comparison presented in Table 4. It can be observed a decrease of both parameters as the length of the perfluorinated alkyl group increases, in agreement with both, previous results [11] and unimolecular reaction rate theories.

The  $C_4F_9OO-NO_2$  bond rupture was studied with the UB3LYP/6-311+G\* method evaluating the energy of the molecule when the bond is elongated and the other parameters relaxed. The dissociation process was calculated evaluating the energy while increasing the  $OO-N$  distance from 1.278 to 4.482 Å. The scan shows the typical energy surface of a simple fission process. A more detailed calculation including the evaluation of vibrational frequencies from 3 Å gave a loose transition state at 3.145 Å of  $C_4F_9OO-NO_2$  bond length. The calculated activation energy found is  $81.3 \text{ kJ mol}^{-1}$  in excellent agreement with the experimental value.

Kirchner et al. [3] have discussed structure–stability relationships to estimate the thermal stability of peroxy nitrates in terms

**Table 2**

Calculated geometric parameters of the most stable conformer.

Geometric parameters					
$C_4F_9OONO_2$	B3LYP6-311+G*	$C_3F_7OONO_2$	B3LYP6-311+G*	$CF_3OONO_2$	GED
Distance (Å)	1.344	Distance (Å)	1.343	C–F	1.322
F–C (mean)		F–C (mean)		O–C	1.378
C–C (mean)	1.568	C–C (mean)	1.564	O–O	1.414
C5–O6	1.389	C4–O5	1.386	O–N	1.523
O6–O7	1.410	O5–O6	1.411	N=O	1.187
O7–N8	1.561	O6–N7	1.560		
N8=O(9–10)	1.182	N7=O(8–9)	1.182		
Angles (°)		Angles (°)			
F–C–F	108.6	F–C–F	108.9	F–C–F	108.8
C2–C3–C4	114.2	C2–C3–C4	116.5		
C4–C5–O6	105.4	C5–C8–O11	107.4	O–O–C	107.7
C5–O6–O7	109.1	C4–O5–O6	109.4	O–O–N	108.4
O6–O7–N8	108.9	O5–O6–N7	108.9		
O7–N8=O9	116.2	O6–N7=O9	116.2		
O7–N8=O10	108.2	O6–N7=O8	108.3		
O9=N8=O10	135.5	O8=N7=O9	135.5	O=N=O	135.2
C2–C3–C4–C5	-166.6				
C3–C4–C5–O6	-170.7	C2–C3–C4–O5	-56.7		
C4–C5–O6–O7	179.2	C3–C4–O5–O6	179.9		
C5–O6–O7–N8	104.7	C4–O5–O6–N7	104.7	$\varphi(C-O-O-N)$	105.1
O6–O7–N8–O10	178.3	O5–O6–N7–O8	178.1	$\varphi(O-O-N=O3)$	178.3
O6–O7–N8–O9	0.7	O5–O6–N7–O9	0.9		

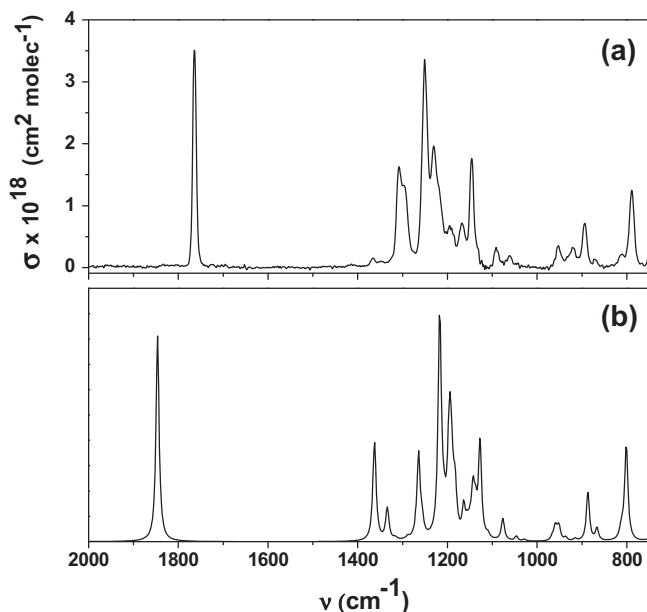


Fig. 4. (a) Experimental and (b) theoretical infrared spectra for  $\text{CF}_3\text{CF}_2\text{CF}_2\text{CF}_2\text{OONO}_2$ .

of the electron density of the carbon atom attached to the  $-\text{OONO}_2$  group; the more electropositive this carbon atom the more stable the O–N bond. We evaluated the electron density of the carbon atom attached to the peroxide group as the Millikan population obtaining +0.12 c.u. for  $\text{C}_4\text{F}_9\text{OONO}_2$  while for  $\text{CF}_3\text{OONO}_2$  (calculated at the same level of theory) this value reaches +0.51 c.u., in agreement with the dissociation activation energies shown in Table 4.

The dependence of the rate constant with total pressure – from 9.0 to 417 mbar – plotted in the inset of Fig. 5, shows that it is more pronounced at low pressures, but beyond 30 mbar its variation falls within the experimental errors. Similar variations are observed in the thermal decomposition of shorter perfluoro alkyl peroxy nitrates.

Table 3

UV absorption cross sections for perfluoro alkyl peroxy nitrates. Experimental errors are showed in brackets.

$\lambda$ (nm)	$\sigma \times 10^{20}$ (cm <sup>2</sup> molecule <sup>-1</sup> )			$\lambda$ (nm)	$\sigma \times 10^{20}$ (cm <sup>2</sup> molecule <sup>-1</sup> )		
	$x = 1$	$x = 3$	$x = 4$		$x = 1$	$x = 3$	$x = 4$
200	220 (10)	167	156 (4)	242		16.7	15.0 (0.3)
202		147	131 (3)	244		15.6	13.6 (0.3)
204		128	115 (3)	246		13.6	12.4 (0.3)
206		111	103 (2)	248		12.7	11.0 (0.2)
208		94.9	88 (2)	250	19 (1)	11.6	9.9 (0.2)
210	110 (10)	81.7	79 (2)	252		10.4	9.1 (0.2)
212		70.1	71 (2)	254		9.39	8.7 (0.2)
214		60.8	63 (1)	256		8.37	8.0 (0.2)
216		52.8	55 (1)	258		7.47	7.2 (0.2)
218		47.1	48 (1)	260	11.5 (0.8)	6.59	6.3 (0.2)
220	58 (4)	42.2	42.0 (0.8)	262		5.85	5.6 (0.2)
222		37.8	37.0 (0.7)	264		5.07	4.9 (0.2)
224		34.8	34.0 (0.7)	266		4.47	4.1 (0.1)
226		31.6	30.0 (0.6)	268		3.89	3.1 (0.1)
228		29.9	27.4 (0.6)	270	5.8 (0.6)	3.24	2.2 (0.1)
230	40 (2)	27.9	25.0 (0.5)	272		2.84	1.7 (0.1)
232		25.9	22.7 (0.5)	274		2.37	1.1 (0.1)
234		24.1	21.0 (0.5)	276		1.98	0.9 (0.1)
236		22.3	19.0 (0.5)	278		1.68	0.8 (0.1)
238		20.0	17.5 (0.5)	280	2.8 (0.5)	1.34	0.7 (0.1)
240	30 (1)	18.7	16.2 (0.5)	282		1.12	0.5 (0.1)

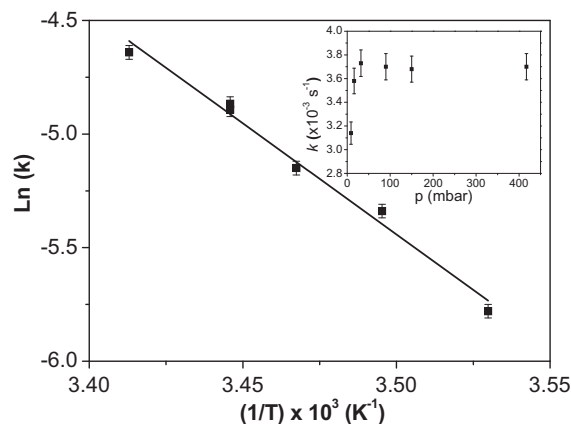


Fig. 5. Temperature dependence of the thermal decomposition of  $\text{CF}_3\text{CF}_2\text{CF}_2\text{CF}_2\text{OONO}_2$  at 9.0 mbar of total pressure. The insert shows the dependence of the rate constant with pressure.

Table 4

Kinetic parameters ( $E_a$  and  $A$ ) of perfluoro alkyl peroxy nitrates as a function of the length of the carbon chain.

	$\text{CF}_3\text{OONO}_2$	$\text{C}_2\text{F}_5\text{OONO}_2$	$\text{C}_3\text{F}_7\text{OONO}_2$	$\text{C}_4\text{F}_9\text{OONO}_2$
$E_a$ (kJ/mol)	90.8	87.7	84.9	$81 \pm 4$
$A$	$1.05 \times 10^{14}$	$3.8 \times 10^{13}$	$1.0 \times 10^{13}$	$3.2 \times 10^{12}$

#### 4.5. Atmospheric implications

The degradation of fluorinated compounds as  $n\text{-CF}_3\text{CF}_2\text{CF}_2\text{CF}_2\text{H}$ , HFC-329p, leads to the formation of perfluorinated radicals, and subsequently to the corresponding perfluoro alkyl peroxy nitrates. The thermal and photochemical lifetime from 0 to 50 km are shown in Fig. 6. The comparison of thermal lifetime profiles for  $\text{C}_x\text{F}_{2x+1}\text{OONO}_2$  calculated for  $x = 1$  [13]; 2 [16]; 3 [11] and 4 (this work), indicates that the thermal lifetime for  $x = 4$  is the shortest, in accordance with the activation energies for the series.

The photochemical lifetime profiles at  $50^\circ$  and  $30^\circ$  S are also presented in Fig. 6. They were calculated using the TUV 4.2

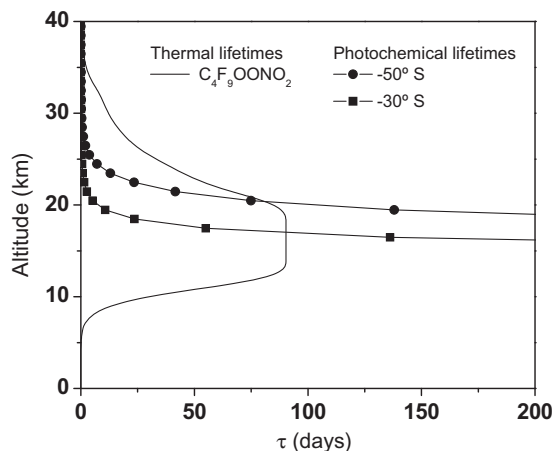


**Fig. 6.** Thermal and photochemical atmospheric lifetimes of  $C_4F_9OONO_2$ . (—): thermal. (—●—): photochemical at  $50^\circ$  and (—■—): photochemical at  $30^\circ$  south latitude.

program [30] as a function of altitude and solar zenith angle. The values presented are the result of the average for four selected days; the solstices and the equinoxes. A pressure independent quantum yield of unity at all wavelengths was assumed.

Comparison between the lifetimes due to thermal and photochemical processes for  $C_4F_9OONO_2$  indicates that the first process controls the atmospheric lifetime. Though at ground level the thermal lifetime is lower than 1 day, at altitudes of the free troposphere it reaches values as long as three months. Beyond 15 km, the photochemical rupture is the dominant process, with lifetime values from 4 months at around 15 km to less than 1 day at altitudes higher than 20 km.

## 5. Conclusions

Synthesis and characterization of the new C4 perfluoro alkyl peroxy nitrates, and its comparison with shorter congeners was performed. This allows an advance in the knowledge of thermal stabilities and atmospheric lifetimes of perfluorinated peroxy nitrates that could be formed in the atmosphere on account of the halocarbons (HCFCs, HFCs, HFES) emitted to the atmosphere.

From the study presented in this paper, it can be concluded that the photochemical lifetime increases with the length of the carbonated chain; while the thermal lifetime follows an opposite behavior. The counteracting effect of these two processes, leads finally to the atmospheric lifetimes of the  $C_xF_{2x+1}OONO_2$  family. Thus, if present in the atmosphere, they should act as a reservoir species of peroxy radicals and  $NO_2$ , mainly in the lower atmosphere.

## Conflict of interest

There are no conflict of interests.

## Acknowledgments

Financial support from SECYT-Universidad Nacional de Córdoba, ANPCyT, and CONICET is gratefully acknowledged. AGB acknowledges the fellowship she holds from CONICET.

## References

- [1] R.K. Talukdar, J.B. Burkholder, A.M. Schmoltner, J.M. Roberts, R.R. Wilson, A.R. Ravishankara, *J. Geophys. Res. [Atmos.]* 100 (1995) 163.
- [2] F. Kirchner, L.P. Thuener, I. Barnes, K.H. Becker, B. Donner, F. Zabel, *Environ. Sci. Technol.* 31 (1997) 1801.
- [3] F. Kirchner, A. Mayer-Figge, F. Zabel, K.H. Becker, *Int. J. Chem. Kinet.* 31 (1999) 127.
- [4] J.M. Roberts, PAN and related compounds, in: R. Koppmann (Ed.), *Volatile Organic Compounds in the Atmosphere*, Blackwell Publishing Ltd., Oxford, UK, 2007.
- [5] R.M. Ravelo, J.S. Francisco, *J. Phys. Chem. A* 112 (2008) 1981.
- [6] C. Buendía-Atencio, V. Leyva, L. González, *J. Phys. Chem. A* 114 (2010) 9537.
- [7] M.P. Badenes, L.B. Bracco, C.J. Cobos, *J. Phys. Chem. A* 115 (2011) 7744.
- [8] R. Kopitzky, M. Beuleke, G. Balzer, H. Willner, *Inorg. Chem.* 36 (1997) 1994.
- [9] M.P. Sulbaek Andersen, M.D. Hurley, T.J. Wallington, J.C. Ball, J.W. Martin, D.A. Ellis, S.A. Mabury, O.J. Nielsen, *Chem. Phys. Lett.* 379 (2003) 28.
- [10] M.P. Sulbaek Andersen, O.J. Nielsen, M.D. Hurley, J.C. Ball, T.J. Wallington, J.E. Stevens, J.W. Martin, D.A. Ellis, S.A. Mabury, *J. Phys. Chem. A* 108 (2004) 5189.
- [11] A.G. Bossolasco, F.E. Malanca, M.A. Burgos Paci, G.A. Argüello, *J. Phys. Chem. A* 116 (2012) 9904.
- [12] C.J. Young, M.D. Hurley, T.J. Wallington, S.A. Mabury, *Chem. Phys. Lett.* 473 (2009) 251.
- [13] A. Mayer-Figge, F. Zabel, K.H. Becker, *J. Phys. Chem.* 100 (1996) 6587.
- [14] R. Kopitzky, H. Willner, H.G. Mack, A. Pfeiffer, H. Oberhammer, *Inorg. Chem.* 37 (1998) 6208.
- [15] F.E. Malanca, M.S. Chiappero, G.A. Argüello, T.J. Wallington, *Atmos. Environ.* 39 (2005) 5051.
- [16] A.G. Bossolasco, F.E. Malanca, G.A. Argüello, *J. Photochem. Photobiol. A: Chem.* 231 (2012) 45.
- [17] O.N. Ventura, M. Kieninger, *Chem. Phys. Lett.* 245 (1995) 488.
- [18] K. Raghavachari, B. Zhang, J.A. Pople, B.G. Johnson, P.M.W. Gill, *Chem. Phys. Lett.* 220 (1994) 385.
- [19] B.G. Johnson, C.A. Gonzalez, P.M.W. Gill, J.A. Pople, *Chem. Phys. Lett.* 221 (1994) 100.
- [20] M.J. Frisch, G.W. Trucks, H.B. Schlegel, G.E. Scuseria, M.A. Robb, J.R. Cheeseman, V.G. Zakrzewski, J.A. Montgomery Jr., R.E. Stratmann, J.C. Burant, S. Dapprich, J.M. Millam, A.D. Daniels, K.N. Kudin, M.C. Strain, O. Farkas, J. Tomasi, V. Barone, M. Cossi, R. Cammi, B. Mennucci, C. Pomelli, C. Adamo, S. Clifford, J. Ochterski, G.A. Petersson, P.Y. Ayala, Q. Cui, K. Morokuma, D.K. Malick, A.D. Rabuck, K. Raghavachari, J.B. Foresman, J. Cioslowski, J.V. Ortiz, A.G. Baboul, B.B. Stefanov, G. Liu, A. Liashenko, P. Piskorz, I. Komaromi, R. Gomperts, R.L. Martin, D.J. Fox, T. Keith, M.A. Al-Laham, C.Y. Peng, A. Nanayakkara, C. Gonzalez, M. Challacombe, P.M.W. Gill, B. Johnson, W. Chen, M.W. Wong, J.L. Andres, C. Gonzalez, M. Head-Gordon, E.S. Replogle, J.A. Pople, *Gaussian 98, Revision A.7*, Gaussian Inc., Pittsburgh, PA, 1998.
- [21] GaussView, Version 5, Roy Dennington, Todd Keith and John Millam, SemicheM Inc., Shawnee Mission, KS, 2009.
- [22] J. Sehested, O.J. Nielsen, T.J. Wallington, *Chem. Phys. Lett.* 213 (1993) 457.
- [23] C.E. Canosa-Mas, A. Vipond, R.P. Wayne, *Phys. Chem. Chem. Phys.* 1 (1999) 761.
- [24] B. Casper, D.A. Dixon, H.-G. Mack, S.E. Ulic, H. Willner, H. Oberhammer, *J. Am. Chem. Soc.* 116 (1994) 8317.
- [25] S.P. Sander, R.R. Friedl, A.R. Ravishankara, D.M. Golden, C.E. Kolb, M.J. Kurylo, R.E. Huie, V.L. Orkin, M.J. Molina, G.K. Moortgat, B.J. Finlayson-Pitts, *Chemical Kinetics and Photochemical Data for Use in Atmospheric Studies*, Jet Propulsion Laboratory, Pasadena, California, 2005.
- [26] L.K. Christensen, T.J. Wallington, A. Guschin, M.D. Hurley, *J. Phys. Chem. A* 103 (1999) 4202.
- [27] F. Zabel, F. Kirchner, K.H. Becker, *Int. J. Chem. Kinet.* 26 (1994) 827.
- [28] J. Sehested, L.K. Christensen, O.J. Nielsen, M. Bilde, T.J. Wallington, W.F. Schneider, J.J. Orlando, G.S. Tyndall, *Int. J. Chem. Kinet.* 30 (1998) 475.
- [29] A.M.B. Giessing, A. Feilberg, T.E. Møgelberg, J. Sehested, M. Bilde, T.J. Wallington, O.J. Nielsen, *J. Phys. Chem.* 100 (1996) 6572.
- [30] S. Madronich, S. Flocke, *The Role of Solar Radiation in Atmospheric Chemistry*, in: P. Boule (Ed.), *Handbook of Environmental Chemistry*, Springer, Heidelberg, 1998, pp. 1–26.